British Journal of Pharmacology

DOI:10.1111/j.1476-5381.2011.01640.x
www.brjpharmacol.org

RESEARCH PAPER

A novel fluorescent histamine H_1 receptor antagonist demonstrates the advantage of using fluorescence correlation spectroscopy to study the binding of lipophilic ligands

Rachel H Rose, Stephen J Briddon and Stephen J Hill

Institute of Cell Signalling, School of Biomedical Sciences, University of Nottingham, Nottingham, UK

Correspondence
Professor SJ Hill, Institute of Cell Signalling, School of Biomedical Sciences, Queen's Medical Centre, Nottingham, NG7 2UH, UK. E-mail: stephen.hill@nottingham.ac.uk

Keywords
histamine; GPCR; fluorescence correlation spectroscopy; fluorescent ligand

Received
25 January 2011
Revised
22 July 2011
Accepted
8 August 2011

BACKGROUND AND PURPOSE
Fluorescent ligands facilitate the study of ligand–receptor interactions at the level of single cells and individual receptors. Here, we describe a novel fluorescent histamine H_1 receptor antagonist (mepyramine-BODIPY630-650) and use it to monitor the membrane diffusion of the histamine H_1 receptor.

EXPERIMENTAL APPROACH
The human histamine H_1 receptor fused to yellow fluorescent protein (YFP) was transiently expressed in CHO-K1 cells. The time course of binding of mepyramine-BODIPY630-650 to the H_1 receptor was determined by confocal microscopy. Additionally, fluorescence correlation spectroscopy (FCS) was used to characterize the diffusion coefficient of the H_1 receptor in cell membranes both directly (YFP fluorescence) and in its antagonist-bound state (with mepyramine-BODIPY630-650).

KEY RESULTS
Mepyramine-BODIPY630-650 was a high-affinity antagonist at the histamine H_1 receptor. Specific membrane binding, in addition to significant intracellular uptake of the fluorescent ligand, was detected by confocal microscopy. However, FCS was able to quantify the receptor-specific binding in the membrane, as well as the diffusion coefficient of the antagonist–H_1 receptor–YFP complexes, which was significantly slower than when determined directly using YFP. FCS also detected specific binding of mepyramine-BODIPY630-650 to the endogenous H_1 receptor in HeLa cells.

CONCLUSIONS AND IMPLICATIONS
Mepyramine-BODIPY630-650 is a useful tool for localizing the H_1 receptor using confocal microscopy. However, its use in conjunction with FCS allows quantification of ligand binding at the membrane, as well as determining receptor diffusion in the absence of significant bleaching effects. Finally, these methods can be successfully extended to endogenously expressed untagged receptors in HeLa cells.

Abbreviations
CHO-K1, Chinese hamster ovary K1 cells; D, diffusion coefficient; DiO, 3,3'-dioctadecyloxacarbcyanine perchlorate; FCS, fluorescence correlation spectroscopy; ROI, region of interest YFP, yellow fluorescent protein

Introduction

The histamine H_1 receptor (nomenclature follows Alexander *et al.*, 2011) is a GPCR that principally couples to the G_q/G_{11} family of heterotrimeric G proteins resulting in activation of PKC and the release of calcium ions from intracellular stores (Hill *et al.*, 1997; Bakker *et al.*, 2002; Leurs *et al.*, 2002). It is a key mediator of allergy and inflammation, and antagonists targeted against this receptor are used commonly in the treatment of allergic conditions such as hay fever (Hill *et al.*, 1997; Bakker *et al.*, 2002; Leurs *et al.*, 2002).

Classically, ligand receptor interactions are studied using radioligand binding or functional assays that require thousands of cells to give a detectable readout (Hill, 2006; Briddon and Hill, 2007; Williams and Hill, 2009; May *et al.*, 2010). However, there is increasing evidence that ligand binding to GPCRs and the subsequent intracellular response is not homogeneous for all cells of a given population (Cordeaux *et al.*, 2008) or even within different membrane regions of the same cell (Ostrom *et al.*, 2001; Ostrom and Insel, 2004; Briddon and Hill, 2007). This heterogeneous receptor distribution, coupled with the recruitment of other signalling proteins to specific membrane microdomains, may have a considerable effect on the final signalling pathway that is activated by an agonist of this receptor in a given cell (Moffett *et al.*, 2000; Ostrom *et al.*, 2001; Briddon and Hill, 2007; Prasad *et al.*, 2009; Williams and Hill, 2009; Kenakin and Miller, 2010; May *et al.*, 2010).

Fluorescent ligands, when combined with highly sensitive imaging technologies such as laser scanning confocal microscopy and fluorescence correlation spectroscopy (FCS), offer the potential to gain detailed insight into the behaviour of ligands at the single cell and membrane microdomain level (McGrath *et al.*, 1996; Briddon and Hill, 2007; Daly *et al.*, 2010). FCS is a technique based on monitoring fluorescence fluctuations created by low concentrations of a diffusing species within a small defined detection volume (~0.2 fL) (Briddon and Hill, 2007; Briddon *et al.*, 2010). Statistical analysis of these fluctuations allows the determination of both the concentration and diffusion coefficient of the fluorescent species present. We have previously used the spatial selectivity of FCS to measure the diffusion of both agonist- and antagonist-occupied receptors in small defined areas of cell membranes (Briddon *et al.*, 2004; Cordeaux *et al.*, 2008). Potentially, such measurements could specifically determine receptor number and diffusion within specific membrane domains. Additionally, the sensitivity of FCS lends itself to quantifying the binding and diffusion characteristics of receptors expressed endogenously at low levels, provided that a suitable fluorescent ligand is available for the receptor of interest. An increasing number of fluorescent ligands for class A GPCRs are available, and they are generally based on a well-characterized ligand coupled to an organic fluorophore (McGrath *et al.*, 1996; Middleton and Kellam, 2005). However, the presence of a linker and a bulky fluorophore substantially increases the molecular size of the final molecule and is likely to lead to pharmacological properties which differ from the parent molecule (Baker *et al.*, 2010). Additionally, changes in the linker composition may also affect the physicochemical properties of the fluorescent ligand. This can be of importance when considering, for example, solubility of the compound and, for imaging applications, its propensity to cross the cell membrane. Under these circumstances, choosing the appropriate methods to assess the binding of ligand is important.

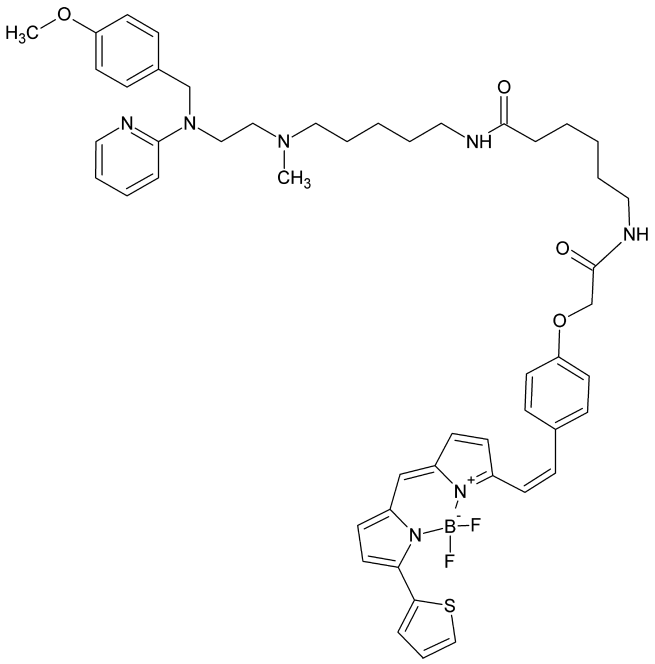

Figure 1
The chemical structure of mepyramine-BODIPY630-650.

This paper describes a new fluorescent analogue of the lipophilic histamine H_1 receptor antagonist mepyramine (mepyramine-BODIPY630-650; Figure 1), and its characterization as a high-affinity fluorescent antagonist for the H_1 receptor. We show its usefulness as a tool for localizing the receptor in single living cells, but also demonstrate that for lipophilic ligands such as this, FCS provides a convenient method for localizing receptor-binding measurements to the membrane of cells expressing the H_1 receptor endogenously or following transfection.

Methods

Generation of receptor constructs

A pcDNA3.1 plasmid containing yellow fluorescent protein (YFP) was kindly provided by Dr Francisco Ciruela (Universitat de Barcelona, Barcelona, Spain). The start codon was mutated to leucine using the QuikChange mutagenesis kit according to the manufacturer's instructions. Polymate Additive was used to improve the success of PCR due to the GC-rich nature of the template, and the complementary oligonucleotide primers CCGCTCGAGACCCCTGGTGAGCA AGGG and CCCTTGCTCACCAGGGGTCTCGAGCGG were used. The YFP fragment containing the mutated start codon was excised using *Xho*I and *Xba*I and inserted downstream of the human histamine H_1 receptor in a pcDNA3.1(+) vector containing a neomycin resistance marker and with the cDNA sequence encoding the myc epitope tag upstream of the receptor sequence. This generated mycH_1–YFP cDNA.

An antagonist binding-deficient variant of the histamine H_1 receptor has previously been described following mutation of phenylalanine-432 to alanine (Bruysters *et al.*, 2004). Therefore, mycH$_1$(F432A)-YFP was generated from mycH$_1$-YFP using the QuikChange mutagenesis kit, Polymate Additive and the complementary oligonucleotide primers CCTCTGCTGGATCCCTTATGCCATCTTCTTCATGGTCATTGC and GCAATGACCATGAAGAAGATGGCATAAGGGATCCAGC AGAGG.

All receptor constructs were sequenced on both strands using automated fluorescent sequencing (University of Nottingham, Nottingham, UK).

Tissue culture and transfection

Chinese hamster ovary cells (CHO-K1) and CHO-K1 cells stably expressing the histamine H_1 receptor (kindly provided by Dr Jillian Baker, University of Nottingham) were grown in Dulbecco's modified Eagle's medium/nutrient mix F12 (DMEM/F12) containing 10% fetal calf serum and 2 mM L-glutamine in a humidified 5% CO_2: 95% air atmosphere at 37°C. HeLa cells were grown under the same conditions, except DMEM supplemented with 10% fetal calf serum and 2 mM L-glutamine was used.

Before transfection, CHO-K1 cells were grown to approximately 70% confluence in eight-well Lab-Tek plates (Nunc Nalgene) in DMEM/F12 containing 10% fetal calf serum and 2 mM L-glutamine. Cells were transfected for 24 h with a total of 0.15 μg per well of DNA using Lipofectamine according to manufacturer's instructions. The transfection mix was aspirated and replaced with DMEM/F12 containing 10% fetal calf serum and 2 mM L-glutamine, and cells were incubated for a further 24 h at 30°C in a humidified atmosphere of 5% CO_2.

Intracellular calcium mobilization assay

To create a stable mixed population of cells expressing the mycH$_1$-YFP or mycH$_1$(F432A)-YFP, CHO-K1 cells were grown to confluence in 75 cm^2 flasks and transfected with 1 μg of the required receptor construct for 24 h using Lipofectamine. Transfected cells were selected by exposure to 1 mg·mL^{-1} neomycin for 3 weeks. Cells were seeded into black, clear-bottomed 96-well plates and grown to confluence overnight. Media was replaced with 100 μL per well HBSS supplemented with 0.1% BSA, 0.5 mM Brilliant Black BN, 2.5 mM probenecid, 0.023% pluronic acid and 2.3 μM Fluo4-AM in the presence or absence of antagonist, and incubated at 37°C for 30–45 min. The highest concentration of histamine (1 mM) was buffered to pH 7.4 prior to serial dilution. Fluorescence intensity was recorded for 200 s using the Molecular Devices Flex Station (Sunnyvale, CA, USA). Histamine was added at the required concentration after 15 s and, in the case of CHO-K1 cells, the ionophore ionomycin (1 μM) was added after 150 s as a means of normalizing the histamine-induced calcium response to variations in cell density.

The histamine response was expressed as a percentage of the maximal change in fluorescence intensity induced by ionomycin, or in the case of HeLa cells, as a percentage of the maximal histamine response. Data are expressed as the mean ± SEM of n independent experiments, each of which was performed in triplicate. Sigmoidal dose response curves were fitted in GraphPad Prism 4 (GraphPad Software, Inc., La Jolla, CA, USA) using the equation:

$$\text{Response} = \frac{E_{max} \times [A]}{[A] + EC_{50}}, \quad (1)$$

where E_{max} is the maximal response to agonist, [A] is the agonist concentration and EC_{50} is the concentration of agonist producing 50% of the maximal response. Mepyramine dissociation constants (K_B) were determined by observing the shift in the histamine concentration–response curve produced by 1 μM mepyramine using the equation:

$$pK_B = \log(DR - 1) - \log[B] \quad (2)$$

where DR (dose ratio) is the ratio of the concentration of histamine required to produce an equivalent functional response in the presence and absence of antagonist, [B] is the molar concentration of the antagonist and K_B is its apparent dissociation constant. Where non-equilibrium dissociation kinetics resulted in suppression of the maximal response to histamine in the presence of antagonists, pK_B was calculated as described in Christopoulos *et al.* (1999).

Confocal imaging

Confocal microscopy was performed using a Zeiss LSM 510 laser scanning microscope with a Zeiss Plan-Apochromat 63 × 1.4NA Ph3 oil immersion objective (Carl Zeiss, Welwyn Garden City, Hertfordshire, UK). For live cell imaging, cells were washed twice with and maintained in sterile HEPES buffered saline solution (HBSS; 10 mM HEPES, 10 mM D-glucose, 146 mM NaCl, 5 mM KCl, 1 mM $MgSO_4$, 1.5 mM $NaHCO_3$, 2 mM sodium pyruvate, 1.3 mM $CaCl_2$; adjusted to pH 7.45) and imaged at 37°C. Dual imaging of YFP with BODIPY630-650 was performed using 488 nm argon and 633 nm helium-neon laser excitation and detected using a 505–550 nm band pass filter and a 650 nm long pass filter. For imaging of BODIPY 630–650 detector gain was fixed at 900 for all experiments and the pinhole diameter to 123 μm (1 airy unit for 633 nm excitation). The amplifier offset was optimized for each experiment at baseline (i.e. prior to addition of mepyramine-BODIPY630-650) to minimize undersaturation of the image.

Fluorescence correlation spectroscopy (FCS)

For CHO-K1 cell experiments, cells were washed and allowed to equilibrate in HBSS, before FCS measurements were performed on the upper cell membrane on a modified Zeiss Confocor 2 system, as previously described (Briddon *et al.*, 2004). Briefly, the volume was positioned in *x*–*y* using a live image from an Axiocam HR camera (Carl Zeiss). Transfected cells were identified using the YFP fluorescence from the histamine H_1 receptor C-terminal YFP construct using a xenon arc lamp. Cells were chosen at a fixed camera exposure to ensure as far as possible a similar expression level in each measurement. Following addition of the fluorescent ligand mepyramine-BODIPY630-530 (3–5 nM), subsequent z-scanning with a 633 nm helium-neon laser allowed positioning of the volume 0.5 μm above the peak intensity of the membrane. Following 8–12 min incubation with mepyramine-BODIPY630-650, FCS readings were taken for

60 s with 633 nm excitation using a laser power of 2.3 kW·cm^{-2}, following a 15 s prebleach at 1.6 kW·cm^{-2}. For measurements of the diffusion of YFP-labelled receptors based on YFP fluorescence, z-scanning with a 514 nm argon laser allowed positioning of the volume on the upper membrane, where FCS readings were taken for 30 s following a 15 s prebleach. Readings were taken using 514 nm laser excitation, at variable laser power, as indicated on the relevant figure. Laser powers were measured at the objective in the absence of sample, using a Fieldmax TO laser power meter fitted with an OP-2 Vis detector (Coherent, Paisley, UK), and subsequent power at sample estimated using the calculated area of the confocal volume from FCS calibration measurements at the appropriate wavelength.

For experiments in HeLa cells, cells were incubated in DMEM containing 1 μM 3,3′-dioctadecyloxacarbcyanine perchlorate (DiO) in the presence or absence of 3 μM cetirizine for 15 min at 37°C, then subsequently washed twice in HBSS before allowing to rest at room temperature for 15 min in HBSS in the presence or absence of 3 μM cetirizine. Mepyramine-BODIPY630-650 (3–5 nM) was added for 5 min prior to recording of fluorescence fluctuations. FCS measurements were taken on a Zeiss LSM510 Confocor 3-enabled confocal microscope using a 40 × 1.2NA c-apochromat water-immersion objective lens. The confocal volume was positioned in x-y on the optical axis of the lens using a live confocal image of the DiO membrane staining (488 nm excitation, emission 505–560 nm band pass, zoom 4). A subsequent scan in the z-axis using low-power 488 nm excitation (0.04 kW·cm^{-2}) to detect the DiO membrane stain allowed precise positioning of the volume 0.5 μm above the upper membrane of the cell, even in the presence of intracellular ligand. Fluctuations were then collected for 20 s following a 10 s prebleach (1.3 kW·cm^{-2}) using 633 nm excitation and emission collected through a 650 nm long pass filter, to detect fluorescent ligand.

In both cases, subsequent analysis and data fitting were performed in Zeiss AIM4.2 software. For measurements of mepyramine-BODIPY630-650, autocorrelation curves were generated and fitted to a model using one three-dimensional diffusion component (with dwell time fixed to that of the ligand measured in HBSS), and one or two two-dimensional diffusion coefficients. For studies of the diffusion of YFP, autocorrelation curved were fitted to a model containing two 2D diffusion coefficients. In both cases, a separate pre-exponential term was added to account for photophysics of the fluorophore, as described in Briddon *et al.* (2010).

Materials

Lipofectamine, Fluo-4AM, Pluronic F-127 and DiO were from Invitrogen (Carlsbad, CA, USA), fetal calf serum was from PAA Laboratories (Pasching, Austria), restriction endonucleases were purchased from Promega (Southampton, UK), QuikChange mutagenesis kit was from Stratagene (La Jolla, CA, USA), Polymate Additive was from Bioline (London, UK) and eight-well Lab-Tek plates were from Nunc Nalgene (Rochester, NY, USA). The fluorescent ligand mepyramine-BODIPY630-650 (Figure 1) was purchased from CellAura Technologies Ltd (Nottingham, UK). All other chemicals were from Sigma Aldrich (Poole, Dorset, UK).

Results

Mepyramine-BODIPY630-650 is a high-affinity H_1 receptor antagonist

Using a stable CHO cell line expressing the H_1 receptor, intracellular calcium mobilization was used to determine the shift in the concentration–response curve to histamine in the presence of 1 μM antagonist and hence, the apparent dissociation constant of the antagonist. Mepyramine-BODIPY630-650 had an apparent dissociation constant (-logK_B = 8.9 ± 0.2, n = 3) that did not significantly differ from that of mepyramine (Figure 2A; -logK_B mepyramine = 8.6 ± 0.3, n = 3). Suppression of the maximal calcium response to histamine was detected in the presence of both 1 μM mepyramine and 1 μM mepyramine-BODIPY630-650, but was greater with the latter (Figure 2A). This is related to the non-equilibrium kinetics of

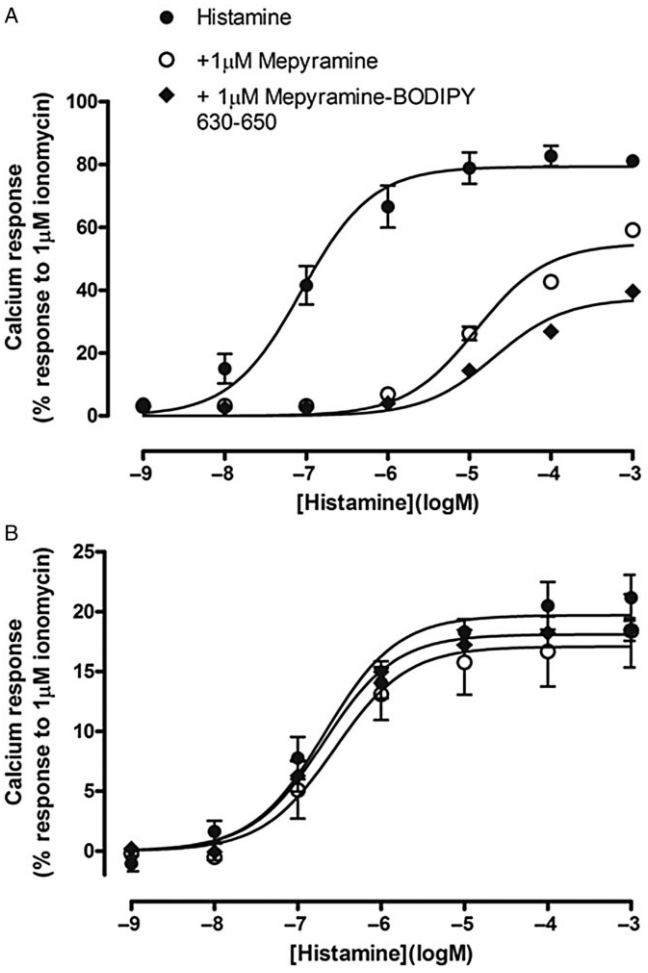

Figure 2

Functional characterization of mepyramine-BODIPY630-650 binding to the H_1 receptor. CHO-K1 cells expressing either (A) wild-type H_1 receptor or (B) mycH_1(F432A)-YFP were preincubated with 1 μM mepyramine or mepyramine-BODIPY630-650 and the intracellular calcium mobilization in response to histamine measured. Responses are expressed as % of the maximal calcium response to ionomycin (1 μM). Data are mean ± SEM of three to four independent experiments, each performed in duplicate.

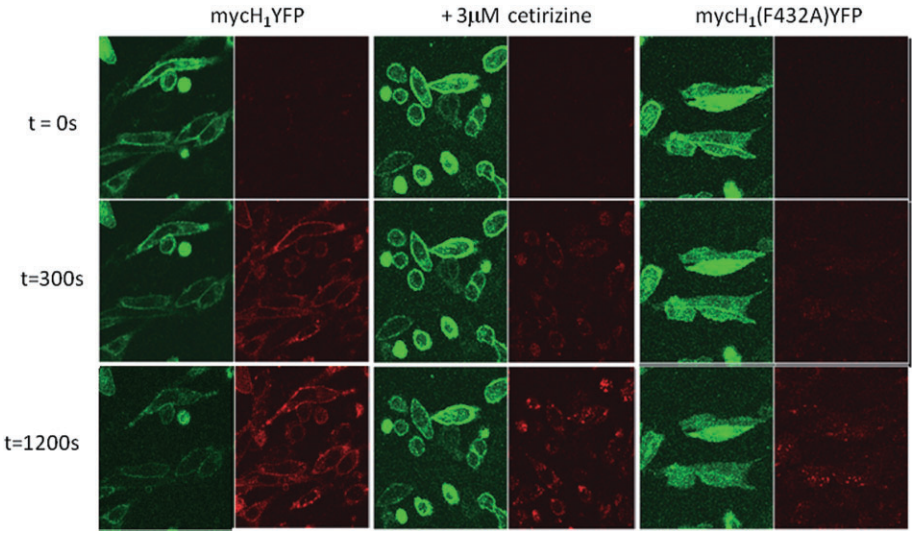

Figure 3

Binding of mepyramine-BODIPY630-650 to mycH$_1$-YFP or mycH$_1$(F432A)-YFP-expressing cells in the absence or presence of the H_1 receptor antagonist cetirizine. CHO-K1 cells were grown to 70% confluence prior to transient transfection with mycH$_1$-YFP or mycH$_1$(F432A)-YFP and incubated at 30°C/5%CO_2 for 24 h before imaging. Cells were maintained in HBSS in the absence (left, right) or presence of 3 μM cetirizine (middle; 30 min preincubation, 37°C) prior to imaging using a Zeiss LSM 510 confocal microscope. Ligand binding was observed for 1200 s following addition of mepyramine-BODIPY630-650 (50 nM) with images taken every 10 s. The left half of each image represents mycH1-YFP (YFP channel) and the right half represents mepyramine-BODIPY630-650 (BODIPY630-650 channel). Images are from a single experiment representative of three independent experiments performed. Images of ligand binding for all transfected receptor constructs were taken using the same microscope settings for both the YFP and BODIPY630-650 channels.

the assay and suggests that mepyramine-BODIPY630-650 has a slower dissociation rate than mepyramine (Christopoulos *et al.*, 1999).

Mutation of phenylalanine-432 in the human histamine H_1 receptor to alanine (F432A mutant) has been reported to prevent the binding of antagonists to the histamine H_1 receptor (Bruysters *et al.*, 2004). The effect of this mutation on the binding of mepyramine and mepyramine-BODIPY630-650, was determined in a mixed population of cells expressing mycH$_1$(F432A)-YFP. In the mixed cell population, the lower maximum response to histamine (compared with the wild-type H_1 receptor, Figure 2A) reflects the heterogeneous nature of the cells transfected with the F432A mutant receptor (Figure 2B). There was no significant change in the EC_{50} or E_{max} of histamine in the presence of either the fluorescent ligand or unlabelled mepyramine (pEC_{50} = 6.6 ± 0.2 in the absence of antagonist; pEC_{50} = 6.6 ± 0.2 or 6.7 ± 0.1 in the presence of 1 μM mepyramine or mepyramine-BODIPY630-650, respectively; E_{max} = 20% of the ionomycin response in the absence of antagonist or 17 ± 3% or 18 ± 1% in the presence of mepyramine or mepyramine-BODIPY630-650 respectively). Both antagonists therefore failed to bind to the F432A mutant H_1 receptor, as previously reported (Bruysters *et al.*, 2004).

Visualization of mepyramine-BODIPY630-650 binding to the H_1 receptor in cell membranes

Binding of 50 nM mepyramine-BODIPY630-650 was measured over a 25 min time course in CHO-K1 cells transiently expressing the H_1 receptor fused to YFP. The YFP fluorescence was used to identify the correct plane of focus for membrane binding prior to addition of mepyramine-BODIPY630-650. Mepyramine-BODIPY630-650 binding largely co-localized with membrane YFP fluorescence in cells expressing mycH$_1$-YFP, but there was some internalization of the fluorescent ligand with time (Figure 3). Membrane binding of mepyramine-BODIPY630-650 was largely prevented by pre-incubation with the H_1 receptor antagonist cetirizine (3 μM), but some internalization of the fluorescent ligand and subsequent accumulation in intracellular regions was detected (Figure 3). No significant membrane binding of mepyramine-BODIPY630-650 was detected to the antagonist binding-deficient mutant mycH$_1$(F432A)-YFP (Figure 3).

To compare the relative amounts of membrane-localized mepyramine-BODIPY630-650 with that present in the cytosol for individual cells, a region of interest (ROI) was drawn around the outside of the cell membrane (ROI_1) and a second one drawn inside the cell membrane (ROI_2). These ROIs were drawn while visualizing the YFP fluorescence of the mycH$_1$-YFP receptor, and allowance was made to account for any movement of the cell during the experiment. Relative fluorescence membrane intensity (relative to cytosolic fluorescence) was then calculated at each time point from the difference in average fluorescence intensity of mepyramine-BODIPY630-650 fluorescence within the two regions (ROI_1 minus ROI_2; Figure 4). A positive relative membrane fluorescence intensity reflected higher levels of membrane binding, whereas negative relative fluorescence intensity values reflected higher levels of intracellular ligand.

Membrane binding of 50 nM mepyramine-BODIPY630-650 to the mycH$_1$-YFP increased steadily with time reaching a

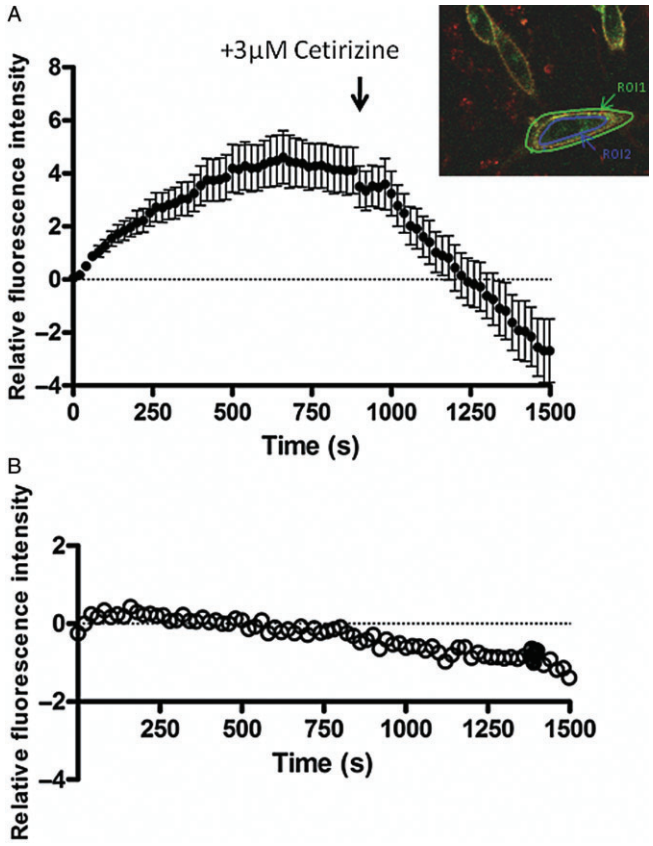

Figure 4

Profiles of the change in fluorescence intensity over time following addition of 50 nM mepyramine-BODIPY630-650. CHO-K1 cells were transiently transfected with (A) mycH$_1$-YFP or (B) mycH$_1$(F432A)-YFP and incubated at 30°C for 24 h prior to imaging. Cells were imaged in HBSS over a time course of 1500 s following the addition of 50 nM mepyramine-BODIPY630-650. For both channels, the laser power, offset and gains were fixed for all experiments and tested constructs. The effect of unlabelled antagonist on mepyramine-BODIPY630-650 binding was determined by addition of 3 μM cetirizine 900 s after the addition of mepyramine-BODIPY630-650 (A; indicated by an arrow). To determine the relative amounts of membrane- and cytosolic- localized mepyramine-BODIPY630-650 at different time points, a ROI was drawn around the outside of the cell membrane (inset; ROI$_1$) and inside the cell membrane (inset; ROI$_2$). ROIs were drawn using fluorescence in the YFP channel. Relative fluorescence intensity was calculated as the difference between the average fluorescence intensity of ROI$_1$ and ROI$_2$. Data represent the mean ± SEM of data from seven cells obtained in three independent experiments.

steady-state plateau after 500 s (Figure 4A). Although the degree of membrane binding (taken as the difference between ROI$_1$ and ROI$_2$) with respect to the cytosolic levels of mepyramine-BODIPY630-650 was relatively low, addition of 3 μM cetirizine after a 15 min exposure to mepyramine-BODIPY630-650 caused a rapid loss of membrane binding and a fall in relative fluorescence intensity to negative values, suggesting that a significant amount of the displaced ligand was rapidly internalized (Figure 4A). Cells expressing mycH$_1$(F432A)-YFP failed to show a rapid membrane binding of 50 nM mepyramine-BODIPY630-650, but instead showed a gradual increase in ligand internalization with time, indicated by a fall in relative intensity values below zero (Figure 4B).

Characterization of fluorescent ligand binding by FCS

Characterization of mepyramine-BODIPY630-650 binding to the mycH1-YFP receptor in CHO cells. FCS allows quantification of receptor–ligand complexes and their diffusion in small areas of cell membrane. The highly localized nature of the measurements is particularly useful in the presence of intracellular ligand, as observed in the confocal experiments with mepyramine-BODIPY630-650. For this reason, we also used FCS to quantify mepyramine-BODIPY630-650-mycH$_1$-YFP complexes and their diffusion in CHO cell membranes. For these experiments, cells transiently expressing mycH$_1$-YFP or mycH$_1$(F432A)-YFP were exposed to 5 nM mepyramine-BODIPY630-650 for 5–15 min. The detection volume was positioned over the cell nucleus in the *x-y* plane and 0.5 μm above the upper membrane peak detected following a fluorescence intensity scan in the *z* plane, and fluorescence fluctuations were collected using a 633 nm helium-neon laser line for excitation. Autocorrelation analysis of these fluctuations resulted in two types of autocorrelation curves containing differing diffusion components. For all autocorrelation curves, a rapidly diffusing component ('L', Figure 5) with a dwell time in the measurement volume of 70–90 μs (diffusion coefficient, D = 2.1–2.7 × 10^{-6} $cm^2 \cdot s^{-1}$) was observed. This represents three-dimensional diffusion of mepyramine-BODIPY630-650 in solution, and is consistent with the diffusion coefficient of the ligand measured directly in HBSS. For each experiment, the dwell time of mepyramine-BODIPY630-650 in HBSS was determined from a calibration read, and fixed as one component in the subsequent analysis. FCS measurements of ligand binding to the mycH$_1$-YFP receptor were subsequently performed on the upper membrane of CHO cells following incubation with mepyramine-BODIPY630-650. In these measurements, in addition to this fast-diffusing free ligand, two slower membrane-bound (two dimensional) diffusion components were detected in 90% of cells (n = 46), subsequently referred to as fast and slow ligand-bound membrane components (LB$_F$ and LB$_S$, respectively, Figure 5A and B). However, in the remaining cells (n = 5; 10% of the total), only free ligand (F) and the fast-diffusing mebrane-bound ligand (LB$_F$) were detectable; this was usually associated with a lower fluorescent intensity at the cell membrane (Figure 5C and D). In cells pre-treated with 3 μM cetirizine, free ligand (L) was detected, but only a single, faster ligand-bound membrane component (LB$_F$) was identified in the majority of cells (66%). Under similar conditions (5 nM mepyramine-BODIPY630-650), the majority of mycH$_1$(F432A)-YFP-expressing cells (66%) exhibited both fast- and slow-diffusing membrane components (LB$_F$ and LB$_S$). The effect of cetirizine treatment and the F432A mutation on both the fast- (LB$_F$) and slow- (LB$_S$) diffusing species has therefore been determined.

In mycH$_1$-YFP-expressing cells, there was a significant reduction in the amount of LB$_S$ detected following both pre-treatment with cetirizine and the introduction of the F432A mutation (P < 0.05, Figure 6A). This reduction was seen both in terms of the reduced proportion of cells displaying this component and also the reduced particle density of those

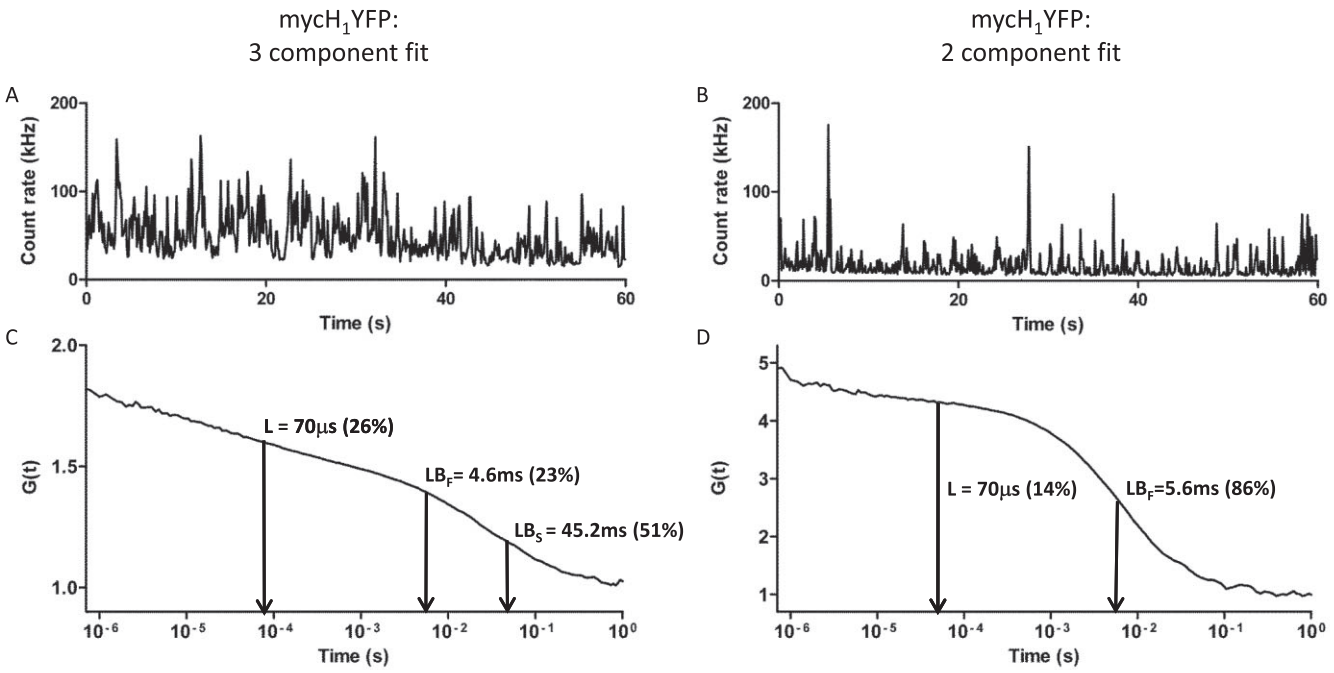

Figure 5

FCS analysis of mepyramine-BODIPY630-650 binding to mycH1-YFP. Examples of FCS analysis of two data sets for the diffusion of 5 nM mepyramine-BODIPY630-650 at the surface of CHO-K1 cells transiently expressing mycH$_1$-YFP are shown. Fluctuations in fluorescence intensity of mepyramine-BODIPY630-650 diffusion (A,C) were analysed by autocorrelation analysis, resulting in generation of autocorrelation curves (B,D). Autocorrelation curves were fit to a three component or two component diffusion models, in which the first component was fixed to the three-dimensional diffusion of the free ligand in solution. The majority of curves were best fit to a three component diffusion model (B), containing fast-moving free ligand (L) and both a fast-moving and slow-moving membrane bound components (LB_F and LB_S respectively). However, others (D) lacked the slower membrane-bound component (LB_S) and were typically associated with a lower count rate.

that do. This is consistent with LB_S representing specific binding of mepyramine-BODIPY630-650 to the H_1 receptor. The diffusion coefficient of the slower diffusing membrane component (LB_S) was not significantly changed following antagonist pretreatment in mycH$_1$-YFP-expressing cells. Interestingly, in mycH$_1$(F532A)-YFP-expressing cells, LB_S had a significantly faster diffusion coefficient (Figure 6B).

In marked contrast to the LB_S component, the amount of the fast LB_F component for cells expressing mycH$_1$-YFP was unaffected by pretreatment with 3 µM cetirizine or the F432A mutation of the receptor (Figure 6C). This strongly suggests that this faster LB_F component represents non-specific binding of mepyramine-BODIPY630-650 to other membrane proteins, or the membrane itself. There was, however, a significant reduction in the diffusion coefficient of the fast membrane-bound component (LB_F), when cells expressing mycH$_1$-YFP were pretreated with 3 µM cetirizine, indicating a slower rate of diffusion, compared with untreated cells. No significant change was seen in cells expressing mycH$_1$(F432A)-YFP (Figure 6D).

Comparison of the diffusion of mycH1-YFP determined directly, with that determined by mepyramine-BODIPY630-650 binding. As a further confirmation that LBs represented specific binding of meyramine-BODIPY630-650, the diffusion of mycH$_1$-YFP receptors expressed in the upper cell membrane of CHO-K1 cells was also determined directly using the fluorescence of the YFP tag on the receptor. If the LB_S component largely represents the membrane diffusion of the H_1 receptor, as hypothesized above, then it would be expected to share a similar diffusion coefficient to that detected for the YFP-labelled receptor. However, in these experiments, the diffusion coefficient of mycH$_1$-YFP determined directly by YFP fluorescence ($5.3 \pm 0.2 \times 10^{-9}$ cm^2·s^{-1}) was significantly faster than the diffusion of the slow component of mepyramine-BODIPY630-650 (LB_S, $D = 3.2 \pm 0.4 \times 10^{-9}$ cm^2·s^{-1}; $P < 0.05$, unpaired *t*-test). One explanation for this difference is differences in the susceptibility to spot photo bleaching of the BODIPY630-650 and YFP fluorophores. As described above, FCS relies on detecting time-dependent fluctuations in fluorescence intensity over time. If a fluorescent particle bleaches (and therefore loses its fluorescence) during its passage through the detection volume, then statistically this will therefore result in an artificially short dwell time in the volume and yield an apparent increase in the diffusion coefficient. If, therefore, YFP has a greater propensity to bleach than BODIPY630-650, then this will present as an increase in the apparent membrane diffusion coefficient relative to that seen for mepyramine-BODIPY630-650. To identify whether this was occurring diffusion coefficients were determined over a range of laser powers, as spot bleaching increases with increasing laser intensity. In cells expressing mycH$_1$-YFP, there was a steep linear increase in diffusion coefficient of the mycH1-YFP when determined using YFP fluorescence directly

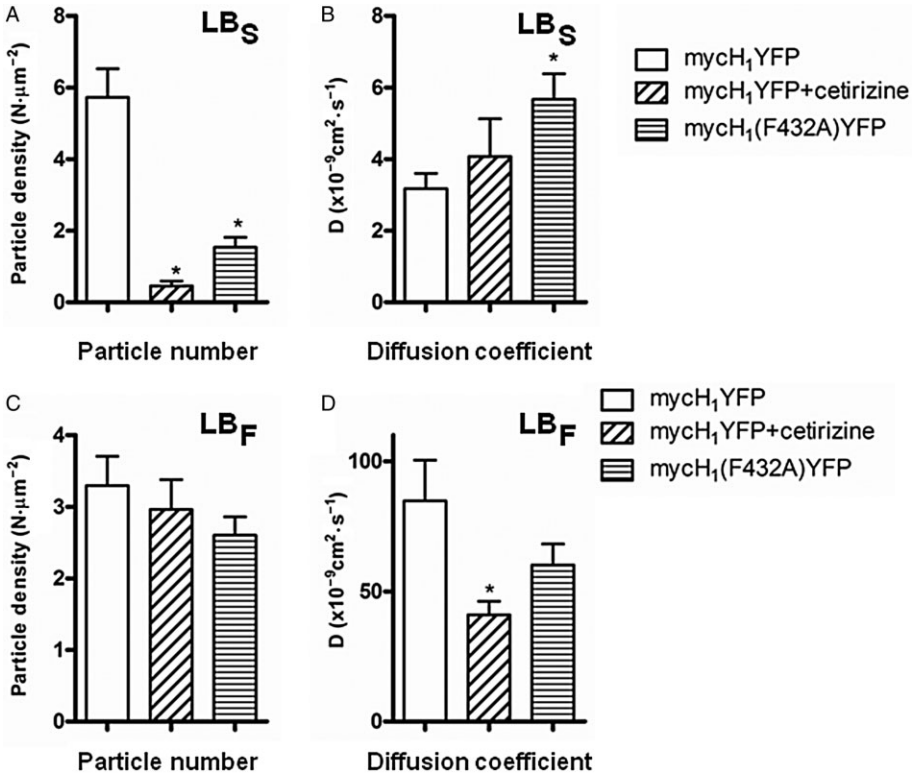

Figure 6

Quantification of mepyramine-BODIPY630-650 binding to mycH$_1$-YFP using FCS. The data show a comparison of the differences in particle density and diffusion coefficient of the fast (LB$_F$) and slow (LB$_S$) components of the mepyramine-BODIPY630-650 obtained by autocorrelation analysis. Particle density (A, C) and diffusion coefficients (B,D) of the slow membrane diffusion component (LB$_S$; A,B) and faster membrane diffusion component (LB$_F$, C,D) are shown for cells transiently expressing the mycH$_1$-YFP receptor in the absence or presence of 3 µM cetirizine or the mycH$_1$(F432A)-YFP receptor. Data represent the mean ± SEM of 39–51 cells from at least three independent experiments. *P < 0.05, significantly different from mycH$_1$-YFP; one-way ANOVA followed by Dunnett's multiple comparison test.

(Figure 7). In contrast, when using mepyramine-BODIPY630-650 to determine diffusion of the mycH$_1$-YFP receptor, there was only a small linear increase in diffusion coefficient as laser power increased. For reference, the laser powers used in previous FCS experiments were 0.34 and 2.33 kW·cm^{-2}, for YFP and BODIPY630-650 respectively.

From these results, it is clear that the diffusion coefficient of mycH$_1$-YFP as detected by YFP fluorescence is significantly more sensitive to the excitation laser power than the slow component of mepyramine-BODIPY630-650 diffusion. Interestingly, both lines converge towards a common point for zero laser power (1.6 ± 0.5 and 2.1 ± 0.7 × 10^{-9} cm^2·s^{-1} for BODIPY and YFP fluorescence respectively at x = 0) that presumably reflects the true diffusion coefficient of the mycH$_1$-YFP receptor protein.

Detecting binding of mepyramine-BODIPY630-650 to the endogenous H1 receptor in HeLa cells. One of the advantages of using a fluorescent ligand in conjunction with FCS is the ability to characterize receptor–ligand interactions at endogenously expressed receptors. This derives from, firstly, the sensitivity of FCS which allows its use at low endogenous levels of expression and secondly, the use of a fluorescent ligand which negates the need for the receptor itself to be labelled. We tested whether mepyramine-BODIPY630-650 was useful for such measurements by assessing its binding to the endogenous H$_1$ receptors, which have previously been shown to exist in HeLa cells (Raymond *et al.*, 1991; Das *et al.*, 2007; Horio *et al.*, 2010).

Initially, we confirmed the presence of functional H$_1$ receptors in HeLa cells by measuring changes in intracellular calcium in response to histamine stimulation. Histamine caused a substantial concentration-dependent increase in intracellular calcium with a log EC$_{50}$ of –8.01 ± 0.05 (n = 6, Figure 8A), which was antagonized by mepyramine with an affinity consistent with the presence of an H$_1$ receptor (apparent log K$_B$ = –9.41 ± 0.17, n = 6). These results are similar to those seen for the mycH$_1$-YFP construct expressed in CHO cells described above, including the depression of the maximum response in the presence of mepyramine.

Subsequently, we used FCS in conjunction with mepyramine-BODIPY630-650 to detect diffusion of the H$_1$ receptor in HeLa cell membranes. As before, FCS measurements were taken 0.5 µm above the upper cell membrane. In the case of HeLa cells, discrete membrane binding of the fluorescent ligand was difficult to detect with confocal imaging due to high intracellular levels of fluorescent ligand (not shown). Accurate positioning of the detection volume on the upper cell membrane was therefore achieved using the non-specific membrane stain, DiO, as a membrane

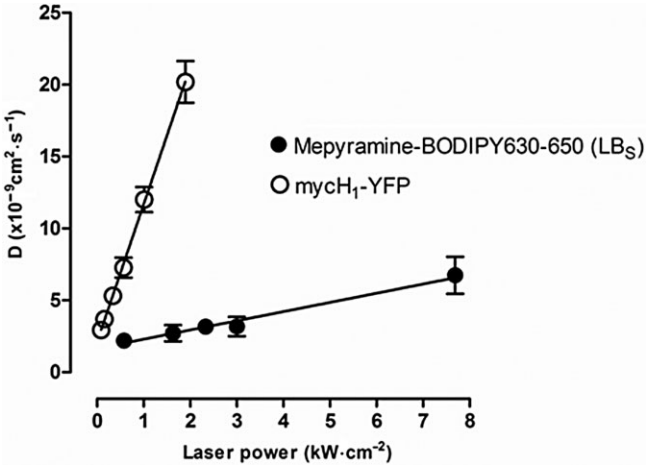

Figure 7

The effect of laser power on the apparent diffusion coefficient of mycH$_1$-YFP detected by FCS using either YFP or mepyramine-BODIPY630-650 fluorescence. The diffusion coefficient (D) of the mycH$_1$-YFP construct in the upper membrane of transiently transfected CHO-K1 cells was measured by FCS using either YFP fluorescence (open circles) or mepyramine-BODIPY630-650 fluorescence (closed circles) at different excitation laser powers. In both cases, there was a clear linear relationship between laser power and diffusion coefficient. A laser power of 0.34 kW·cm^{-2} was routinely used in measurements of YFP diffusion, whereas a laser power of 2.33 kW·cm^{-2} was normally used in measurements of mepyramine-BODIPY630-650 diffusion. Data represent the mean ± SEM of 8–46 individual cells from at least three independent experiments.

marker (see Methods section). Following incubation with mepyramine-BODIPY630-650 (3 nM, 5 min, 22°C), FCS measurements showed a fast-moving membrane-bound component in addition to that of free ligand (D = 20.8 ± 1.6 × 10^{-9} cm^2·s^{-1}, n = 25, Figure 8B). In a small number of cells (10/25) a slower membrane-bound component was also detected (D = 2.8 ± 0.6 × 10^{-9} cm^2·s^{-1}). Preincubation of HeLa cells with the non-fluorescent H_1 antagonist cetirizine (3 μM, 10 min, 37°C), significantly reduced the amount of the fast-moving component that was detected (P < 0.01, Figure 8A), indicating that this represents the diffusion of endogenous H_1 receptor occupied by fluorescent antagonist. Interestingly, the diffusion co-efficient of the membrane-bound fluorescent ligand was significantly faster in cells pre-incubated with cetirizine (D = 34.5 ± 0.5 × 10^{-9} cm^2·s^{-1}). The slow-diffusing component was also seen in the presence of cetirizine (6/12 cells) suggesting this represents predominantly non-specific binding.

Discussion

This paper describes the characterization of a novel fluorescent mepyramine analogue, mepyramine-BODIPY630-650 that maintains high affinity for the histamine H_1 receptor. We also demonstrate the use of this ligand, in conjunction with the technique of FCS, to determine the diffusion characteristics of the H_1 receptor in small areas of the cell membrane, and apply this to the receptor in both model and endogenously expressed systems.

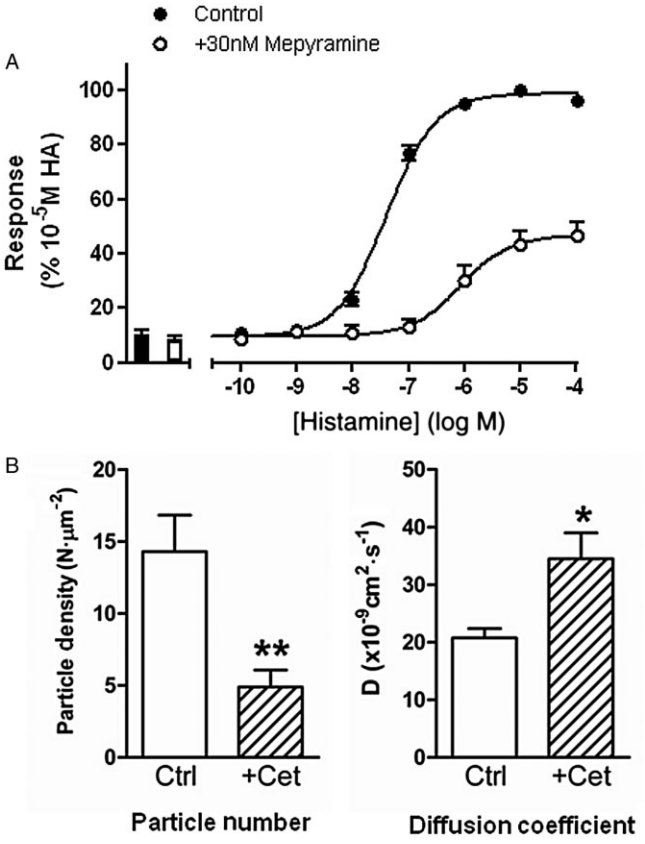

Figure 8

Detection of the endogenous H_1 receptor on HeLa cells by (A) measuring histamine-induced changes in intracellular calcium and (B) binding of meyramine-BODIPY630-650 using FCS. (A) Changes in intracellular calcium in HeLa cells in response to histamine in the absence and presence of mepyramine (30 nM, 45 min, 37°C) were assessed, as described in the Methods section. Basal values in the absence (closed bars) and presence (open bars) of mepyramine are shown. Data are normalized to the control response to 10^{-5} M histamine, and are the mean ± SEM of five independent experiments performed in quadruplicate. (B) HeLa cells were stained with DiO in the absence (Ctrl) and presence of 3 μM cetirizine (+ Cet). Subsequently, cells were incubated with 3 nM mepyramine-BODIPY630-650 (5 min, 22°C) and FCS measurements performed +0.5 μm above the upper cell membrane. Left, the amount of fast-moving membrane-bound ligand in control cells and those preincubated with cetirizine was quantified by curve fitting, as described in the Methods. Right, the diffusion coefficient of the fast-moving membrane bound component was also determined from the same data. Data shown are the mean ± SEM of measurements from 12–26 cells, obtained in at least five independent experiments. *P < 0.05 and **P < 0.01, significantly different from control, unpaired Student's t-test.

Fluorescent ligands for class A GPCRs are becoming more widely available, and it is evident that the correct combination of pharmacophore, conjugation position, fluorophore and linker are necessary to produce a ligand with all of the desired pharmacological, physicochemical and photophysical properties (McGrath *et al.*, 1996; Middleton and Kellam, 2005; Baker *et al.*, 2010). The lipophilic fluorophore BODIPY630-650 has been successfully used previously in such ligands, and its red-shifted excitation–emission spectra

is compatible with multicolour imaging, and help reduce photo-toxicity and autofluorescence during live cell imaging experiments (Briddon *et al.*, 2004; Baker *et al.*, 2010). In this case, attaching BODIPY630-650 to mepyramine via an alkyl linker results in a fluorescent ligand, which shows an affinity for the H_1 receptor, similar to that of its parent pharmacophore. Interestingly binding was prevented by mutation of phenylalanine-432 to alanine, suggesting the fluorescent ligand uses at least some of the same amino acid interactions as mepyramine.

Binding of meyramine-BODIPY630-650 to the H_1 receptor was detected by co-localization with the YFP-tagged H_1 receptor in CHO-K1 cells using standard confocal imaging. The specific nature of this binding was confirmed in experiments that showed binding was prevented both by preincubation with the non-fluorescent antagonist cetirizine (3 μM) or mutation of the antagonist ligand binding site in the mycH$_1$(F432A)-YFP receptor construct. However, in all cases, intracellular accumulation of mepyramine-BODIPY630-650 was detected over a period of 25 min incubation, most likely related to the lipophilic nature of the ligand, which would allow it to readily penetrate the cell membrane. Interestingly, there appeared to be a lower intracellular level of binding of mepyramine-BODIPY630-650 in the mycH$_1$(F432A)-YFP cell line, which probably indicates that some of the intracellular binding of mepyramine-BODIPY630-650 in cells expressing the wild-type receptor is to intracellular H_1 receptors on route to or from the cell membrane. This is also consistent with the partial intracellular distribution of YFP fluorescence in the wild-type cells (Figure 3). Ligand internalization has previously been reported for other fluorescent ligands and appears to be at least partially related to the physicochemical properties of the ligand (Baker *et al.*, 2003; Daly and McGrath, 2003). The significant uptake of the fluorescent ligand into cells does, however, make it difficult to properly quantify the degree of receptor binding at the plasma membrane using conventional confocal microscopy. A previous study using [^{3}H]-mepyramine in intact U373MG cells also found that this radiolabelled ligand caused significant labelling of intracellular sites due to penetration into the cell (Hishinuma and Young, 1995).

This difficulty led us to develop an alternative approach to detect and quantify membrane binding of mepyramine-BODIPY630-650, namely the biophysical technique of FCS. FCS is a highly sensitive confocal imaging technique, which uses a fixed but highly localized confocal detection volume (Muller *et al.*, 2003; Elson, 2004). This confocal volume illuminates a region of ~1 × 0.3 μm (a membrane area of ~0.2 μm^2), and can therefore be placed with a high degree of precision on the plasma membrane. FCS also relies on time-dependent fluctuations in fluorescent intensities within the confocal volume, which are greater at low concentrations (Muller *et al.*, 2003; Elson, 2004; Briddon and Hill, 2007), and is therefore best suited to low ligand concentrations and low expression levels of the receptor. From the point of view of cell-penetrating lipophilic ligands, such as meyramine-BODIPY630-650, this means that FCS offers significant advantages over standard confocal imaging. Firstly, the precision of placement allows a minimal amount of cytoplasm to be present in the detection volume and secondly, the low concentration of ligands used should reduce the amount of cytosolic uptake. Although mepyramine-BODIPY630-650 was able to enter the cell cytosol in significant amounts, it remained possible to detect the specific receptor-bound component on the cell membrane by FCS. Autocorrelation analysis identified two putative membrane-bound components of mepyramine-BODIPY630-650 binding with differing diffusion coefficients. The first was a fast-diffusing component (LB_F; D = 40–80 × 10^{-9} cm^2·s^{-1}), which appeared to represent largely non-specific binding, and the second was a slow component (LB_S; D = 3–6 × 10^{-9} cm^2·s^{-1}) which was identified as the diffusion of a mepyramine-BODIPY630-650-myc-H_1-YFP receptor complex. The evidence that LB_S represents specific binding of mepyramine-BODIPY630-650 to the histamine H_1 receptor is compelling and comes from the marked reduction in particle number of this component following both mutation of the antagonist binding site or prior treatment of cells with cetirizine. Similarly, the lack of displacement the LB_F component of mepyramine-BODIPY630-650 in the presence of cetirizine, or the lack of effect of the F432A mutation is consistent with it being non-specific binding. However, it was notable that there was a significant reduction in the diffusion coefficient of the LB_F component following cetirizine treatment, which suggests that there may be also a receptor-specific binding contribution in this component of binding in addition to non-specific binding. It is possible in this situation that the displacement of any specific receptor binding by cetrizine in this fraction is offset by a change in the oligomeric composition of the ligand-bound diffusing species, leading to an equal number of slower diffusing non-specific binding protein complexes. It is also worth pointing out that a diffusion coefficient of 3–6 × 10^{-9} cm^2·s^{-1} for receptor-specific component (LB_S) is too slow to represent a single receptor protein and probably equates to the presence of the H_1 receptor in a macromolecular complex as has been observed for other GPCRs (Briddon and Hill, 2007).

To validate our measurements of H_1 receptor diffusion using mepyramine-BODIPY630-650, we compared our measurements with the diffusion of the mycH$_1$-YFP receptor measured directly through excitation and detection of the YFP fluorescence. The diffusion coefficient of the mycH$_1$-YFP receptor construct was expected to be the same whether detected by specific binding of mepyramine-BODIPY630-650 or fluorescence of the YFP fusion protein. However, this was not the case, and a more rapid rate of diffusion was detected by FCS based on YFP fluorescence (D = 5.3 × 10^{-9} cm^2·s^{-1}) than the diffusion of mepyramine-BODIPY630-650 (for the specific binding component, LB_S, D = 3.2 × 10^{-9} cm^2·s^{-1}). This difference can be explained by the fact that YFP has a greater sensitivity to spot bleaching than mepyramine-BODIPY630-650 (Figure 7), which may be due to differences in the photostability of YFP and BODIPY630-650. It may also be related to the kinetic nature of ligand binding since a ligand binds reversibly to the receptor, and so, there is potential for a continual dissociation and association of ligand with the receptor within the detection volume that limits the exposure of the fluorophore to laser light (McGrath *et al.*, 1996). Additionally, since the measurements are taken in the continued presence of free fluorescent ligand, any bleached ligand can be readily replaced. Importantly, at low laser powers, the diffusion coefficients detected by the different fluorophores were very similar. In the case of the H_1 receptor the predicted

diffusion coefficient under conditions of zero spot bleaching by both fluorophores is between 1.6 and 2.1 × 10^{-9} $cm^2 \cdot s^{-1}$ (Figure 7). This also supports the idea that LB_S represents specific receptor-bound ligand, The apparent increase in the diffusion coefficient observed using YFP fluorescence is not seen for all fluorescent proteins. There is also evidence that for both adenosine A_3 receptors and β_3-adrenoceptors, that GFP does not spot bleach as significantly as YFP, and in these cases, diffusion coefficients determined by ligand binding and receptor diffusion are equivalent (S.J. Briddon and S.J. Hill, unpubl. obs.).

The applicability of the FCS method for quantifying the binding of lipophilic fluorescent ligands was further demonstrated using HeLa cells. Several previous studies have demonstrated endogenous expression of the H_1 receptor in HeLa cells at levels ranging from 130 to 700 $fmol \cdot mg^{-1}$ protein (Raymond *et al.*, 1991; Das *et al.*, 2007; Horio *et al.*, 2010). This was confirmed in our HeLa cells, where histamine induced a mepyramine-sensitive increase in intracellular calcium. As with transiently transfected CHO cells, detecting membrane binding of mepyramine-BODIPY630-650 using standard confocal imaging was difficult because of high levels of intracellular ligand (data not shown). Indeed, for FCS measurements membrane staining with the carbocyanine dye, DiO, was used to ensure correct positioning of the detection volume on the upper membrane. However, there was a clear cetirizine-sensitive component of binding seen following autocorrelation analysis of FCS data from HeLa cells incubated with a low concentration of mepyramine-BODIPY630-650. These mepyramine-BODIPY630-650/H_1 receptor complexes showed a much faster diffusion than the LB_S component detected in CHO cells (although slower than the LB_F component). One possible explanation for this is that the H_1 receptor is present in HeLa cell membranes in a different macromolecular complex or membrane domain compared with CHO cells. For instance, the presence of H_1 receptor in a caveolae or lipid rafts in CHO cells has previously been demonstrated (Self *et al.*, 2005), and it may be that in HeLa cells, the receptor is in non-raft domains, which have a faster movement. Receptor localization and complexing may also be influenced by the presence of the YFP on the receptor C-terminus in CHO cells, although the mass difference itself is unlikely to be enough for such a difference in diffusion coefficient. Interestingly, there was a slower diffusing membrane-bound component of fluorescent mepyramine in HeLa cells, but this appeared to represent non-specific binding. This suggests that the membrane proteins or lipids which contribute to non-specific binding are also different in HeLa cells.

Fluorescent ligands are emerging as an important tool in studying receptor pharmacology at the single cell and subcellular level, providing a more detailed insight than is possible with radioligand binding studies (Briddon and Hill, 2007; Cordeaux *et al.*, 2008; Leopoldo *et al.*, 2009; Daly *et al.*, 2010). They also offer the potential to image native receptors in cells and tissues, without the need for transfection as required for genetically encoded fluorescent protein labels. In this study, we have also shown that even a highly lipophilic fluorescent ligand (with an increased propensity to enter the cytosol) can be characterized and quantified by FCS; and importantly, this is true at both artificially and endogenously expressed receptors. The ability to detect specific receptor diffusion using a lipophilic ligand is relevant to a number of targets in which only lipophilic ligands are available such as the fatty acid receptors. Differences between the sensitivity to spot bleaching of BODIPY630-650 and YFP explain the differences in rates of diffusion of mycH$_1$-YFP detected using the different fluorophores and suggest that mepyramine-BODIPY630-650 provides a better tool for measurement of the true diffusion coefficient of the histamine H_1 receptor.

In conclusion, we have demonstrated that mepyramine-BODIPY630-650 can be used to label the human H_1 receptor in single living cells. Despite its lipophilic properties that lead to substantial uptake of the fluorescent ligand into the cytosol, the technique of FCS can be used to study the ligand-binding and diffusional properties of the human H_1 receptor in discrete membrane microdomains of living cells. This suggests that this approach might be equally amenable to the study of GPCRs for which only highly lipophilic ligands are available, for example, fatty acid receptors and cannabinoid receptors. We have shown that the diffusional characteristics of the ligand-bound H_1 receptor provide a more reliable measure of the actual diffusion coefficient because the fluorescence of mepyramine-BODIPY630-650 is much less susceptible to spot bleaching following laser excitation. However, this will only be the case when the fluorescent ligand dissociates from the receptor slowly. It is therefore very important that the photochemical, pharmacological and physicochemical properties are all taken into consideration when designing fluorescent ligands for use with FCS.

Acknowledgement

We thank the MRC for financial support (grant # G0800006). Rachel Rose was supported by a British Pharmacological Society A J Clark Studentship.

Conflict of interest

SJH is a director of the University of Nottingham spin out company CellAura Technologies that provided the fluorescent ligand.

References

Alexander SPH, Mathie A, Peters JA (2011). Guide to Receptors and Channels (GRAC), 5th Edition. Br J Pharmacol 164 (Suppl. 1): S1–S324.

Baker JG, Hall IP, Hill SJ (2003). Pharmacology and direct visualisation of BODIPY-TMR-CGP: a long acting fluorescent beta2-adrenoceptor agonist. Br J Pharmacol 139: 232–242.

Baker JG, Middleton R, Adams L, May LT, Biriddon SJ, Kellam B *et al.* (2010). Influence of fluorophore and linker composition on the pharmacology of fluorescent adenosine A1 receptor ligands. Br J Pharmacol 159: 772–786.

Bakker RA, Timmerman H, Leurs R (2002). Histamine receptors: specific ligands, receptor biochemistry and signal transduction. Clin Allergy Immunol 17: 27–64.

Briddon SJ, Hill SJ (2007). Pharmacology under the microscope: the use of fluorescence correlation spectroscopy to determine the properties of ligand-receptor complexes. Trends Pharmacol Sci 28: 637–645.

Briddon SJ, Middleton RJ, Cordeaux Y, Flavin FM, Weinstein JA, George MW *et al*. (2004). Quantitative analysis of the formation and diffusion of A1-adenosine receptor-antagonist complexes in single living cells. Proc Natl Acad Sci U S A 101: 4673–4678.

Briddon SJ, Hern JA, Hill SJ (2010). Use of fluorescence correlation spectroscopy to study the diffusion of GPCRs. In: Poyner DR, Wheatley M (eds). G Protein Coupled Receptors: Essential Methods. Wiley-Blackwell: Chichister, pp. 169–196.

Bruysters M, Pertz HH, Teunissen A, Bakker RA, Gillard M, Chatelain P *et al*. (2004). Mutational analysis of the histamine H1-receptor binding pocket of histaprodifens. Eur J Pharmacol 487: 55–63.

Christopoulos A, Parsons AM, Lew MJ, El-Fakahany EE (1999). The assessment of antagonist potency under conditions of transient response kinetics. Eur J Pharmacol 382: 217–227.

Cordeaux Y, Briddon SJ, Alexander SP, Kellam B, Hill SJ (2008). Agonist-occupied A3 adenosine receptors exist within heterogeneous complexes in membrane microdomains of individual living cells. Faseb J 22: 850–860.

Daly CJ, McGrath JC (2003). Fluorescent ligands, antibodies, and proteins for the study of receptors. Pharmacol Ther 100: 101–118.

Daly CJ, Ross RA, Whyte J, Henstridge CM, Irving AJ, McGrath JC (2010). Fluorescent ligand binding reveals heterogeneous distribution of adrenoceptors and 'cannabinoid-like' receptors in small arteries. Br J Pharmacol 159: 787–796.

Das AK, Yoshimura S, Mishima R, Fujimoto K, Mizuguchi H, Dev S *et al*. (2007). Stimulation of histamine H_1 receptor up-regulates histamine H1 receptor itself through activation of receptor gene transcription. J Pharmacol Sci 103: 374–382.

Elson EL (2004). Quick tour of fluorescence correlation spectroscopy from its inception. J Biomed Opt 9: 857–864.

Hill SJ (2006). G-protein-coupled receptors: past, present and future. Br J Pharmacol 147: S27–S37.

Hill SJ, Ganellin CR, Timmerman H, Schwartz JC, Shankley NP, Young JM *et al*. (1997). International union of pharmacology. 13. Classification of histamine receptors. Pharmacol Rev 49: 253–278.

Hishinuma S, Young JM (1995). Characteristics of the binding of [^{3}H]-mepyramine to intact human U373MG astrocytoma cells: evidence for histamine-induced H_1-receptor internalisation. Br J Pharmacol 116: 2715–2723.

Horio S, Fujimoto K, Mizuguchi H, Fukui H (2010). Inerleukin-4 up-regulates histamine H1 receptors by activation of H1 receptor gene transcription. Naunyn Schmiedebergs Arch Pharmacol 381: 305–313.

Kenakin T, Miller LJ (2010). Seven transmembrane receptors as shapeshifting proteins: the impact of allosteric modulation and functional selectivity on new drug discovery. Pharmacol Rev 62: 265–304.

Leopoldo M, Lacivita E, Berardi F, Perrone R (2009). Developments in fluorescent probes for receptor research. Drug Discov Today 14: 706–711.

Leurs R, Church M, Taglialatela M (2002). H1-antihistamines: inverse agonism, anti-inflammatory actions and cardiac effects. Clin Exp Allergy 32: 489–498.

May LT, Holliday ND, Hill SJ (2010). The evolving pharmacology of GPCRs. In: Gilchrist A (ed.). GPCR Molecular Pharmacology and Drug Targeting – Shifting Paradigms and New Directions. Wiley: Hoboken, NJ, pp. 17–60.

McGrath JC, Arribas S, Daly CJ (1996). Fluorescent ligands for the study of receptors. Trends Pharmacol Sci 17: 393–399.

Middleton RJ, Kellam B (2005). Fluorophore-tagged GPCR ligands. Curr Opin Chem Biol 9: 517–525.

Moffett S, Brown D, Linder ME (2000). Lipid-dependent targeting of G proteins into rafts. J Biol Chem 275: 2191–2198.

Muller JD, Chen Y, Gratton E (2003). Fluorescence correlation spectroscopy. Methods Enzymol 361: 69–92.

Ostrom RS, Insel PA (2004). The evolving role of lipid rafts and caveolae in G protein-coupled receptor signaling: implications for molecular pharmacology. Br J Pharmacol 143: 235–245.

Ostrom RS, Gregorian C, Drenan RM, Xiang Y, Regab JW, Insel PA (2001). Receptor number and caveolar co-localization determine receptor coupling efficiency to adenylyl cyclase. J Biol Chem 276: 42063–42069.

Prasad R, Paila YD, Jafurulla M, Chattopadhyay A (2009). Membrane cholesterol depletion from live cells enhances the function of serotonin 1A receptors. Biochem Biophys Res Commun 389: 333–337.

Raymond JR, Albers FJ, Middleton JP, Lefkowitz RJ, Caron MG *et al*. (1991). 5-HT_{1A} and histamine H_1 receptors in HeLa cells stimulate phosphointositide hydrolysis and phosphate uptake via distinct G protein pools. J Biol Chem 266: 372–379.

Self TJ, Oakley SM, Hill SJ (2005). Clathrin-independent internalization of the histamine H_1-receptor in CHO-K1 cells. Br J Pharmacol 146: 612–624.

Williams C, Hill SJ (2009). GPCR signaling: Understanding the pathway to successful drug discovery. Methods Mol Biol 552: 39–50.